Excitation levels and magic numbers of small parahydrogen clusters ($N \leqslant 40$)

Rafael Guardiola[1] and Jesús Navarro[2,a)]
[1]*Departamento de Física Atómica y Nuclear, Facultad de Física, 46100 Burjassot, Spain*
[2]*IFIC, CSIC-Universidad de Valencia, Apdo. 22085, 46071 Valencia, Spain*

(Received 14 February 2008; accepted 7 March 2008; published online 9 April 2008)

The excitation energies of parahydrogen clusters have been systematically calculated by the diffusion Monte Carlo technique in steps of 1 molecule from 3 to 40 molecules. These clusters possess a very rich spectra, with angular momentum excitations arriving up to $L=13$ for the heavier ones. No regular pattern can be guessed in terms of the angular momenta and the size of the cluster. Clusters with $N=13$ and 36 are characterized by a peak in the chemical potential and a large energy gap of the first excited level, which indicate the magical character of these clusters. From the calculated excitation energies, the partition function has been obtained, thus allowing for an estimate of thermal effects. An enhanced production is predicted for cluster sizes of $N=13$, 31, and 36, which is in agreement with the experiment. © *2008 American Institute of Physics*.
[DOI: 10.1063/1.2903462]

I. INTRODUCTION

Small $(p\text{-}H_2)_N$ clusters of parahydrogen have been produced in a cryogenic free jet expansion and studied by Raman spectroscopy.[1] The $Q(0)$ Raman line of the H_2 monomer is shifted as the number N of molecules in the cluster changes, thus providing a method to identify the cluster mass. The first seven resolved peaks next the monomer line have been assigned to clusters with $N=2,\ldots,8$ molecules. Although in that experiment the resolution was not enough to resolve larger sizes, broad maxima were observed at $N\approx 13$ and 33, and perhaps 55, which have been interpreted as a propensity for geometric shell structures. Indeed, classical static[2–4] and molecular dynamics[4,5] results, which are based on the generic Lennard–Jones interaction potential, indicate that the expected structures for such clusters are the so-called Mackay icosahedra,[6] which exhibit some magic sizes (13,33,55,…) related to the packing of molecules in closed icosahedral arrangements. A very complete discussion of classical geometrical patterns and their relation to the interaction features can be found in Ref. 7 and references therein. However, quantum effects play a major role in $p\text{-}H_2$ clusters, like in their helium droplets analogs. The path integral Monte Carlo (PIMC) simulations of Sindzingre *et al.*[8] have shown that indeed the superfluid fraction in $p\text{-}H_2$ clusters with 13 and 18 molecules become large at temperatures below $T\simeq 2$ K. This prediction prompted both experimental[9] and theoretical[10–13] research of small clusters consisting of $p\text{-}H_2$ molecules surrounding a carbonyl sulfide chromophore, confirming the existence of a superfluid response.

Quantum Monte Carlo (QMC) methods have been widely used in recent years as a theoretical tool to study $p\text{-}H_2$ clusters. Several QMC techniques have been employed to calculate their properties, namely, variational Monte Carlo, diffusion Monte Carlo (DMC),[14–18] PIMC,[8,19–22] reptation Monte Carlo,[23] and path integral ground state (PIGS) Monte Carlo.[24] Only some specific values of the number N of constituents have been considered in the past, which are related to the expected Mackay icosahedra structures. More recently, systematic calculations as a function of the number of molecules in the cluster have been performed. The ground state energies and the one-body densities of $p\text{-}H_N$ clusters have been calculated by the DMC technique in steps of 1 molecule from $N=3$ to 50,[17] by the PIGS technique from $N=2$ to 20,[24] and by the PIMC from $N=5$ to 40.[21,22] The calculations show that $(p\text{-}H_2)_N$ clusters exhibit a clear geometrical order, with the molecules occupying concentric spherical shells, which could be related to some polyhedric arrangement. The apparent incompatibility between the large superfluid fractions and the structured radial distribution densities has been recently clarified[21,22] by PIMC calculations which show that superfluidity is localized at the surface of the clusters.

Whereas up to $N\simeq 22$, these calculations are substantially in agreement, for heavier clusters there are noticeable differences between DMC and PIMC results, particularly for $N\geqslant 26$. PIMC chemical potentials show very prominent peaks at $N=26$, 29, 34, and 39, in contrast to a smoother behavior obtained with DMC. These differences subsist even after an improved DMC calculation,[18] and seem to be related to thermal effects. According to Mezzacapo and Boninsegni[21] they should be associated with a coexistence of solidlike and liquidlike phases, with a dominance of the latter at low T, as a result of both the zero-point motion and quantum permutation exchanges. However, thermal effects could manifest in enhanced stability thresholds at finite temperature, similarly to what has been observed in ^{4}He droplets.[25] Such droplets are definitely liquidlike and, nevertheless, they exhibit some magic numbers, which are not related to enhanced ground state binding energies at specific values of N. Instead, they are stability thresholds related to

a)Electronic mail: navarro@ific.uv.es.

the cluster sizes at which excited levels cross the chemical potential curve and become stabilized.[26] An analysis of the possible existence of similar enhanced stabilities in p-H_2 could be helpful to interpret the experimental results of Ref. 1.

The purpose of the present article is to provide an accurate microscopic description of the ground state and the low-lying excited levels of $(p\text{-}H_2)_N$ clusters. In the past, the excited states of the $N=7$ cluster were analyzed by McMahon *et al.*[27] Here, we present a systematic calculation of excitations with angular momentum from $L=0$ to 13 for clusters with $N=3,\ldots,40$. For a given L-state, the Schrödinger equation has been solved by means of stochastic DMC techniques using the pairwise potential determined by Buck *et al.*,[28] hereafter referred to as BHKOS. Another popular choice is the potential due to Silvera and Goldman,[29] hereafter referred to as SG. Both potentials combine *ab initio* calculations with properties of the gas (or solid) as well as experimental information from collisions. The main difference among them is that SG contains a repulsive long-range term (c_9/r^9) to approximate the effective potential in a solid. As shown in Ref. 18, the BHOKS potential provides more binding than the SG one, and the BHOKS chemical potential is slightly higher than the SG one.

This paper is organized as follows. In Sec. II, technical details of the DMC calculations are given for the ground state and low-lying excited states. The energy levels of $(p\text{-}H_2)_N$ clusters are presented and discussed in Sec. III. In Sec. IV, the partition functions are obtained from the excitation energies, and they are applied to the calculation of the abundances in free jet expansions of parahydrogen clusters. A summary and some general conclusions are finally given in Sec. V.

II. THE DIFFUSION MONTE CARLO METHOD

The DMC method[30] solves the imaginary-time Schrödinger equation for a function $f(\mathcal{R},t)=\Phi_{\rm var}(\mathcal{R})\Psi(\mathcal{R},t)$ which is the product of the importance-sampling wave function $\Phi_{\rm var}$ and the true ground state wave function Ψ. The variable $\mathcal{R}$ represents the set $(\mathbf{r}_1,\ldots,\mathbf{r}_N)$ of $3N$ coordinates of the N molecules which form the drop. The solution for f is obtained by constructing an approximate small-time Green's function $G(\mathcal{R},\mathcal{R}',\tau)$ which serves to advance f by a small-time step τ,

$$f(\mathcal{R}',t+\tau)=\int d\mathcal{R}G(\mathcal{R}',\mathcal{R},\tau)f(\mathcal{R},t). \tag{1}$$

An initial set of walkers $\{\mathcal{R}_1,\mathcal{R}_2,\ldots,\mathcal{R}_{N_w}\}$ is created to represent the function $f(\mathcal{R},0)$ at the initial time. After many repeated applications of the short-time approximate Green's function, all components of the starting wave function orthogonal to the ground state wave function disappear and the contributions of the other eigenstates go exponentially to zero as the time goes to infinity. The remaining set of walkers then provides a valid representation of the converged solution. In order to have a good statistical accuracy, it is convenient to continue the application of the Green's function along a very large number of time steps and accumulate the resulting set of walkers. Then, the mixed estimators of the physically interesting quantities, such as the total energy, can be computed. Of course, since the walkers are strongly correlated, a block average is carried out in order to estimate the variance.

Our ground state calculations are based on a Jastrow-like importance-sampling wave function depending on just two parameters.

$$\Phi_{\rm var}=\prod_{i<j}^{N}\exp\left(-\frac{1}{2}\left(\frac{r_{ij}}{b}\right)^5-\frac{r_{ij}}{p}\right), \tag{2}$$

where $r_{ij}=|\mathbf{r}_i-\mathbf{r}_j|$ is the distance between the pair (i,j). Once the variational parameters for each value of N were determined, DMC calculations were carried out with very small real-time steps $(5\times10^{-5}-1\times10^{-5}\ \mathrm{K}^{-1}$, for the light and heavier clusters, respectively) and very long number of evaluation steps. Notice that the Bose symmetry of the above guiding wave function is not modified in the DMC process. The inclusion of triplet correlations in the importance-sampling function leads to a noticeable improvement of the variational energies, as shown in Ref. 18. However, the DMC energies are essentially the same as those obtained with only two-body correlations, with slightly more binding in the heavier clusters. The main difference lies in the reduction in the standard deviation by typically a factor of 2.

Importance-sampling wave functions with a nonzero angular momentum may equally well be considered and, correspondingly, the initial state will be an admixture of eigenstates of a specified angular momentum L. A convenient trial function with angular momentum L is as follows:

$$\Phi_{\rm var}^{(L)}(\mathcal{R})=\sum_{i=1}^{N}\mathrm{Re}\{|\mathbf{r}_i-\mathbf{R}_{\rm cm}|^L Y_{LL}(\bar{\omega}_i)\}\Phi_{\rm var}(\mathcal{R}), \tag{3}$$

where $\bar{\omega}_i$ stands for the spherical angles of the vector $\mathbf{r}_i-\mathbf{R}_{\rm cm}$ which defines the position of the ith particle with respect to the center-of-mass coordinate $\mathbf{R}_{\rm cm}=\Sigma_i\mathbf{r}_i/N$, and Y_{LM} is a spherical harmonic. Note that the sum over all the constituent particles and the subtraction of the center-of-mass coordinate $\mathbf{R}_{\rm cm}$ are required to maintain the Bose symmetry and the translational invariance, respectively. Again, the application of the imaginary-time Green's function will select the lowest eigenstate in the subspace of angular momentum L, the remaining contributions being exponentially suppressed as the time increases. The prefactor entering Eq. (3) is identical to zero when $L=1$. In that case, we have used

$$\Phi_{\rm var}^{(1)}(\mathcal{R})=\sum_{i=1}^{N}\mathrm{Re}\{|\mathbf{r}_i-\mathbf{R}_{\rm cm}|^3 Y_{11}(\bar{\omega}_i)\}\Phi_{\rm var}(\mathcal{R}). \tag{4}$$

A similar procedure to deal with L-states has been used in Ref. 27 for the $N=7$ cluster, and in Ref. 26 for ^{4}He droplets.

Certainly, the trial function for $L\neq0$ states is not positive definite and, consequently, cannot be interpreted as a probability distribution function. We have used the so-called fixed-node approximation[31] assuming that the nodal surfaces are fixed by the importance-sampling function. In this approximation, an exact energy for the lowest angular momen-

tum L state is, in fact, not obtained. The improved variational wave function and the corresponding mixed estimator of the energy, which is derived, does, however, provide a variational upper bound.

Besides the excited states with angular momentum L, one should also consider vibrational excitations characterized by a radial quantum number n. In short, let us represent each state by (n,L). With the previous trial wave function, the DMC method selects the lowest eigenstate $(0,L)$ in the subspace of angular momentum L. A useful estimate of the energies of the average vibrational excitations $(n \geqslant 1,L)$ in each L subspace is obtained by using sum rules,[32,33] which only require the knowledge of the lowest L-state wave functions. Consider the exact lowest state for a given angular momentum L and the full set of eigenstates of this subspace in order of increasing energy, represented by $\Psi_0^{(L)}$ and $\{\Psi_n^{(L)}, E_n^{(L)}\}$, respectively, where $n=0,1\ldots$, is the vibrational quantum number. Let $Q(\mathcal{R})$ be an arbitrary operator, assumed to be scalar under rotations, for which the sum rule of order p is given by

$$M_p^{(L)}[Q] = \sum_{(n,\ell)\neq(0,L)} (E_n^{(\ell)} - E_0^{(L)})^p |\langle \Psi_n^{(\ell)}|Q|\Psi_0^{(L)}\rangle|^2, \tag{5}$$

where the sum extends over all eigenstates of the Hamiltonian with the exception of the lowest energy state $(0,L)$ of angular momentum L. An upper bound to the energy of the first excited state of the subspace L is obtained as

$$E_1^{(L)} - E_0^{(L)} \leqslant \frac{M_1^{(L)}[Q]}{M_0^{(L)}[Q]}, \tag{6}$$

which involves the energy weighed and the nonenergy weighed sum rules. Using the completeness relation of the set of functions $\{\Psi_n^{(L)}\}$, they can be written as

$$M_0^{(L)}[Q] = \langle \Psi_0^{(L)}|Q^2|\Psi_0^{(L)}\rangle - |\langle \Psi_0^{(L)}|Q|\Psi_0^{(L)}\rangle|^2, \tag{7}$$

$$M_1^{(L)} = \frac{\hbar^2}{2m}\langle \Psi_0^{(L)}|\sum_{i=1}^{N} |\nabla_i Q|^2|\Psi_0^{(L)}\rangle. \tag{8}$$

The computation of these expressions only requires a knowledge of the lowest state wave function of the angular momentum L subspace.

Here, we present the results for the first vibrational state of the subspace $L=0$, employing a general monopolar operator

$$Q(\mathcal{R}) = \sum_{p=1}^{5} c_p \sum_{i<j} r_{ij}^p. \tag{9}$$

The parameters c_p have been optimized so as to obtain the lowest upper bound to the first excited state. Notice that the excitations obtained are approximate because mixed matrix elements are used to calculate the required sum rules, so that strict variational character is lost.

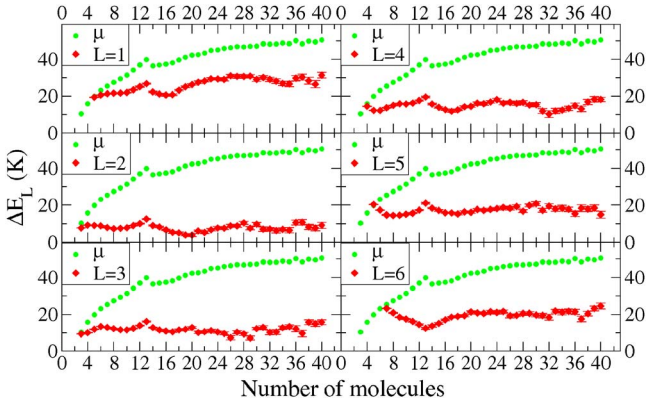

FIG. 1. (Color online) Excitation energies (in K) of $(p\text{-}H_2)_N$ clusters as a function of the number N of constituents for states $(0,L)$ with $L=1-6$. The chemical potential $\mu(N)$ is also displayed to indicate the stability limit.

III. THE ENERGY LEVELS OF PARAHYDROGEN CLUSTERS

Once calculated for each cluster the ground state $E_0^{(0)}(N)$ and the excited-state energies $E_0^{(L)}(N)$ and $E_1^{(0)}(N)$, the excitation energies are defined as

$$\Delta E_{L\neq 0}(N) = E_0^{(L)}(N) - E_0^{(0)}(N), \tag{10}$$

$$\Delta E_0(N) = E_1^{(0)}(N) - E_0^{(0)}(N). \tag{11}$$

They are plotted as a function of N in Figs. 1–3. For the sake of clarity, we have separately displayed them for each value of L in Figs. 1 and 2 and the full spectra are shown in Fig. 3. The chemical potential or dissociation energy

$$\mu(N) = E_0^{(0)}(N-1) - E_0^{(0)}(N), \tag{12}$$

defined as the difference between the ground state energies of the neighboring clusters, has also been plotted in all cases. Indeed, the chemical potential defines the energetic region in which excited states are stable. Only stable states have been plotted in Figs. 1–3.

As previously discussed in Refs. 17 and 18, the most prominent result regarding the chemical potential is the enhanced stability of the cluster $N=13$, which confirms its magical character. A mild peak also appears at $N=36$, but

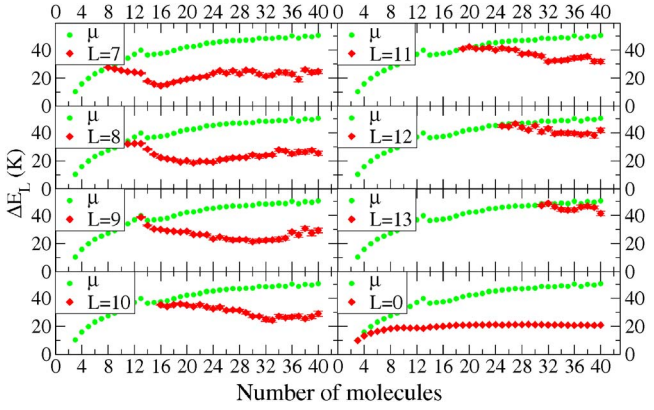

FIG. 2. (Color online) Excitation energies (in K) of $(p\text{-}H_2)_N$ clusters as a function of the number N of constituents for states $(0,L)$ with $L=7-13$ and the vibrational state $(1,L)$ with $L=0$. The chemical potential $\mu(N)$ is also displayed to indicate the stability limit.

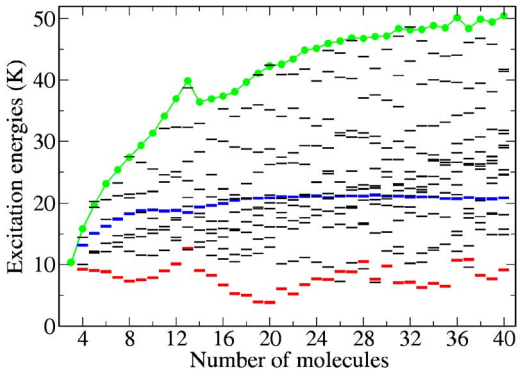

FIG. 3. (Color online) Excitation energies (in K) of $(p\text{-}H_2)_N$ clusters as a function of the number of constituents. The chemical potential $\mu(N)$ (green dots) is also displayed to indicate the stability limit. Levels ($n=0$, $L=2$) and ($n=1$, $L=0$) are plotted in red and blue, respectively.

one cannot exclude that it could simply be a statistical fluctuation. An additional confirmation of its magicity will be given later on. In contrast, PIMC calculations of Refs. 21 and 22 at $T=1$ and 0.5 K, respectively, showed an enhanced stability at $N=13$, 26, 29, 34, and 39.

The main characteristics of the spectra displayed in Figs. 1 and 2 can be summarized as follows. All clusters exhibit stable excitations for $L=2$, 3, and 0 at $N=3$ and onward. The next excited level with $L=4$ starts to be bound at $N=4$, the following levels with $L=5$ and 1 appear at $N=6$. The next $L=6,\ldots$, levels appear at regularly increasing size thresholds. In the considered size range the highest stable excited level corresponds to $L=13$, which appears at $N=31$ and onward. The quadrupolar $L=2$ excitation is the lowest one for all sizes, except at $N=26$, 28, 29, and 37, for which the octupolar $L=3$ state lies at a slightly lower energy. The excitations with $L\geqslant 7$ do not cross each other: The higher the angular momentum is, the higher the excitation energy. The vibrational excitation energies of the state $(n=1,L=0)$ present a smooth behavior as a function of N, apart from a mild minimum at $N=13$. We have not pushed our calculations to the vibrational states $(1,L\neq 0)$. Presumably, they would also present a monotonic behavior with respect to their corresponding $(0,L)$ states. In contrast, the excitation energies of the states $(n=0,L\neq 0)$ have a nonmonotonic behavior with N.

The $N=13$ cluster is very peculiar. Its excitation energies present a prominent peak for the states with $L=1-5$, a prominent minimum for $L=6$, and a pronounced change of trend for $L=7$, 8, and 9. This cluster has no stable excited states for $L\geqslant 9$. No other enhanced bumps appear up to $N=40$. Such a behavior is related to the truly magic character of this size. Its enhanced stability results in a repulsion of the excitations, similarly to what has been observed in classical Lennard–Jones calculations.[4,34] The prominent minimum found for $L=6$ at $N=13$ means that this value of the angular momentum is also special. A similar phenomenon was observed in the study of doped parahydrogen clusters $CO@(p\text{-}H_2)_N$ by reputation QMC calculations,[23] where the time-correlation functions of the various multipole moments in the rotating-axes frame have been computed. A persistent crystal structure for $N=12$ and a persistent time correlation of the $L=6$ multipole has been observed by these authors. Their explanation for these facts was based in the property that the only non-null multipolar moments for the $N=13$ cluster with icosahedral symmetry are $L=6$ and $L=10$.

TABLE I. Cluster with $N=7$. The DMC results of Ref. 27 are compared to the present results. All energies are in K.

	McMahon *et al.*	Present results
$E_0^{(0)}$	−98.89(15)	−98.76(1)
μ	25.90(15)	25.37(2)
ΔE_2	8.3(3)	7.92(13)
ΔE_3	13.2(2)	12.92(17)
ΔE_5	15.4(2)	14.74(18)

To the best of our knowledge, there are only two available calculations of excited states of parahydrogen clusters. Costa and Clary[35] performed a calculation in a large basis for both the dimer and the trimer by using the surface potential of Schaeffer and Meyer.[36] No bound 0^+ excitation was found for the trimer, in contrast to our findings. There is no contradiction because of the variational character of the results of Costa and Clary. The other calculation for the cluster with $N=7$ is due to McMahon *et al.*[27] These authors have performed a DMC calculation using the BHKOS interaction and a trial wave function for L-excited states analogous to Eq. (3). It can be seen in Table I that their calculations and ours are in substantial agreement within at most two standard deviations.

Our calculated DMC excitation energies are collected in Fig. 3, omitting error bars for the sake of clarity. The obtained spectrum for each $(p\text{-}H_2)_N$ cluster is *complex*, in the sense that it does not resemble any of the simple models of excitations. The states with $L=2$ are the lowest lying, apart from the few cases mentioned before. It is worth mentioning the presence of relevant energy gaps at $N=13$ and $N=36$, in coincidence with peaks in the chemical potential. Both facts indicate a magical character of these clusters. Note that analogous energy gaps have been determined in classical Lennard–Jones clusters.[4]

There is almost no information, neither experimental nor theoretical, of the spectrum of clusters weakly bound by van der Waals-like interactions. An indirect determination of the $(p\text{-}H_2)_2$ dimer excitations has been reported in Refs. 37–39. These interesting experiments refer to the absorption of infrared radiation by parahydrogen gas at 20 K, slightly above the triple point. Just focusing on the region around the $Q_1(0)$ line, there has been observed an *absence* of absorption at exactly the frequency of the free $Q_1(0)$ line, and the presence of two satellites at energies above and below the free parahydrogen frequency, interpreted as a signal of the dimer excited states. In practice, absorption experiments provide an indirect way of detecting the two-body ground state $p\text{-}H_2-p\text{-}H_2$ and measuring its spectrum.

In the case of ^{4}He droplets, an indirect determination of their excitation energies results from the temperature-dependent analysis of the production abundances of such clusters in ultrasonic expansion of pressurized gas.[26] Sudden jumps have been observed in the quantum partition function

at cluster sizes which can just accommodate one more additional stable excitation. The nice agreement between the experimental magic sizes and theoretical stability thresholds provides a confirmation of the calculated energy levels of these clusters.

In principle, one could expect some parallelism between the spectra of ^{4}He droplets and those made of parahydrogen: Both constituents are bosons and the interaction is rather similar. However, our calculations rule out such an analogy, as helium clusters present regularly spaced spectra. In contrast, no simple pattern can be guessed for the spectra of parahydrogen clusters. Only the excitation energy of the $L=0$ level has a smooth behavior with the number of p-H_2 molecules, with a small inflection at $N=13$. Its value is roughly constant near 20 K, quite far away from the dissociation limit, in contrast 10 the analogous level in ^{4}He droplets which is close to the dissociation limit.

The $(n=0,L>1)$ of ^{4}He excitations correspond to surface modes, described by ripplonlike oscillations with radial frequencies given by[40–42]

$$\omega = \left[\frac{\sigma_0}{m\rho_0 R_0^3} L(L-1)(L+2) \right]^{1/2}. \tag{13}$$

Certainly, the smooth behavior related to the angular momentum dependence $[L(L-1)(L+1)]^{1/2}$ does not emerge from our calculated spectra of p-H_2 clusters. These frequencies were corrected by Tamura[43] to include finite size effects. The corrected expression reproduces very well the calculated DMC spectra of helium clusters[26] but not the present spectra of p-H_2 clusters.

The excitation energy of the translationally invariant *forbidden* 1 mode, which requires a nodal surface in the radial coordinate space, has a quite high energy compared to the *allowed* levels (2,3,…), like in the case of helium droplets. Nevertheless, its energy is again far away from the dissociation limit, in contrast to the case of ^{4}He clusters. With respect to the variation with the number of molecules, it is noticeably smoother than the levels of low angular momentum (up to $L=4$) but reveals a prominent bump near $N=13$.

At the light of our calculations, we infer a coexistence of liquid and crystal structure near $N=13$, the liquid part being responsible for the $L=2,3,\ldots$, excitations, and the crystal part responsible for the $L=6$ excitation. The region around $N=13$ where the energy of the $L=6$ mode decreases up to $N=13$ and afterward increases up to a plateau will correspond to a partial icosahedral symmetry. We have analyzed the known crystal structures related to Lennard–Jones clusters reported in the Cambridge cluster data base,[44] by computing the multipolar moments. There are three significant cases worth mentioning. First, the $N=19$ cluster, for which the multipolar moments $L=3$ and $L=4$ are null and for which we obtain a very low $L=2$ excitation and much higher $L=3$ (a peak) and $L=4$. Second, the $N=26$ case, whose first non-null multipole is $L=3$ and appears in our calculations with a minimum for this excitation. Finally, the $N=38$ cluster, whose first non-null multipole is $L=4$ appearing again in our calculations as a valley around this value of the number of constituents. In conclusion, even if we do not find a simple or familiar model to describe the excitations of parahydrogen clusters, some aspects of the spectrum are qualitatively described by assuming a coexistence of liquid and solid phases.

IV. THERMAL EFFECTS AND MAGIC NUMBERS

The knowledge of the full spectra allows us to analyze different thermal effects by means of the partition function. In particular, in this section, we consider the expectation value of the temperature-dependent energy $E(T)$ and the effect of excited states on the production abundances of clusters in free jet expansion of pressurized gas.

The partition function of each cluster is expressed as the product

$$\Xi_N = Z_N \xi_N \tag{14}$$

of the center-of-mass (Z_N) and internal (ξ_N) partition functions. The former can be written as

$$Z_N = \left(\frac{NmkT}{2\pi\hbar^2} \right)^{3/2}. \tag{15}$$

The internal partition function is given in terms of bound state energy levels E_j of the state $j=(n,L)$ of the N-molecule cluster by

$$\xi_N = \sum_j g_j(N) \exp\left[-\frac{E_j(N)}{kT} \right], \tag{16}$$

where the degeneracy factor for the state with the radial quantum number n and angular momentum L is given by $g_j=2L+1$.

By using the notation of Sec. III, Eqs. (10) and (11), the internal partition function may be written in a computationally convenient form

$$\xi_N = \exp\left[-\frac{E_0^{(0)}(N)}{kT} \right] \left[1 + \sum_L (2L+1) \exp\left[-\frac{\Delta E_L(N)}{kT} \right] \right], \tag{17}$$

where $\Delta E_L(N)$ are the excitation energies for angular momentum L, and the statistical factor has been written in the explicit form $(2L+1)$.

The internal energy of a given cluster at a temperature T is given by

$$E_N(T) = E_0^{(0)}(N) + \frac{1 + \Sigma_L (2L+1) \Delta E_L(N) e^{-\Delta E_L(N)/kT}}{1 + \Sigma_L (2L+1) e^{-\Delta E_L(N)/kT}}. \tag{18}$$

Sizable thermal effects on the energy values will start to appear at temperatures close to the energy of the first excited state. Thus, at $T=1$ K, the energy changes are minimal, with a maximum of 0.4 K for $N \simeq 20$, related to the minimum of ΔE_2 (see Fig. 1). The energy of the other clusters remains practically unaltered and, consequently, the chemical potential at $T=1$ K has practically the same shape as at $T=0$. This observation is interesting in relation to the PIMC calculations, which have been carried out at $T=0.5$ K (Ref. 22) and $T=1$ K.[21] The series of peaks observed in the PIMC chemical potential as a function of the number of molecules is not reproduced by the present extension of DMC to $T=1$ K. Although different interactions have been used in these calcu-

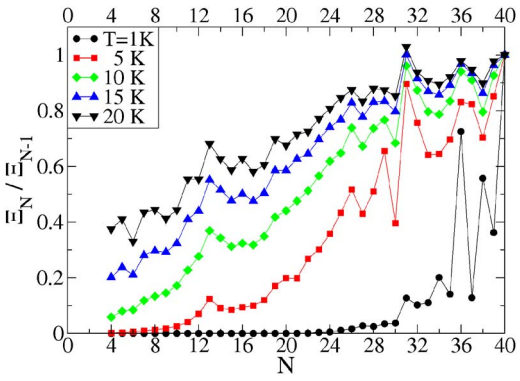

FIG. 4. (Color online) The ratio of the partition functions Ξ_N/Ξ_{N-1} is plotted vs N for several values of temperature: 1, 5, 10, 15, and 20 K. The scale has been arbitrarily fixed at $N=40$.

lations, namely, BHKOS in DMC and SG in PIMC, we do not expect this as the origin of the differences. Indeed, DMC results using both interactions[18] give substantially the same chemical potential shape, apart from the mentioned mild peak at $N=36$, not visible with the SG interaction.

On the other hand, the effect of the temperature on the mechanism by which clusters are formed in the free jet expansion turns out to be very interesting. The analysis which follows is similar to the one carried out for helium droplets[25,26] which explained the experimentally observed anomalously high production rates of clusters with a specific number of constituents; the anomalies being related to the excitation spectrum of the clusters and not to a magical character.

Let us assume that cluster growth is dominated by the chemical equilibrium reaction

$$(\text{p-H}_2)_{N-1} + \text{p-H}_2 + X \rightleftharpoons (\text{p-H}_2)_N + X, \tag{19}$$

where X is a spectator particle required to fulfill the energy and momentum conservation laws. The related equilibrium constant is independent of the spectator particle and is given by a quotient of partition functions

$$K_N = \frac{\Xi_N}{\Xi_{N-1}\Xi_1}. \tag{20}$$

The equilibrium constant is dominated by the quotient Ξ_N/Ξ_{N-1}, which is conveniently written as

$$\frac{\Xi_N}{\Xi_{N-1}} = \left(\frac{N}{N-1}\right)^{3/2} e^{\mu(N)/kT} \frac{1+\Sigma_L g_L e^{-\Delta E_L(N)/kT}}{1+\Sigma_L g_L e^{-\Delta E_L(N-1)/kT}}. \tag{21}$$

Neither the chemical potential nor the excitation energies are smooth functions of N, as has been show in Fig. 3. One can expect that the above quotient will reflect such a nonmonotonic behavior as jumps at particular values of N. The quotient of partition functions Ξ_N/Ξ_{N-1} is displayed in Fig. 4 as a function of N for several values of temperature, lower than the source temperatures of Ref. 1, about 40 K. As these ratios span several orders of magnitude as T varies, we have arbitrarily given the value 1 to the case $N=40$.

Clearly pronounced peaks are observed at $N=13$, 31, and 36, and less pronounced at $N=26$. Other peaks exist, such as $N=19$ and $N=29$, but they only appear at specific values of T. The pronounced peaks give an explanation of the experimentally determined production peaks at $N=13$ and 33. It should be mentioned that the relation between the Raman shift and the number of molecules of the clusters in the work of Tejeda *et al.*[1] is an *extrapolation* from small values of N, and the position of the peak at $N=33$ may be imprecise. It is worth noticing that the last value is halfway between the theoretical peaks at $N=31$ and $N=36$ related to an enhanced production.

V. CONCLUSIONS

In this work, we have determined the excited-state energy levels of parahydrogen clusters containing up to 40 molecules by means of a DMC calculation based on an importance-sampling function with a nonzero angular momentum L plus the fixed-node approximation. A variational upper bound has been obtained for the lowest-lying energy of a given L-state. Bound excited states have been found for states $(n=0,L=1-13)$ and $(n=1,L=0)$, the size threshold for binding increases as L increases. It turns out that the spectra are complex in the sense that no simple pattern can be guessed to fit them as a function of the angular momentum of the state and the size number. In particular, and contrary to what happens in the analogous system of helium droplets, the liquid drop model formula is excluded. Perhaps an appropriate description could be found considering the interplay between solid and liquid structures.

The $N=13$ and $N=36$ clusters are magic, as indicated by the existence of peaks in the chemical potential in coincidence with energy gaps for their first low-lying excited state, relative to their neighbors.

The spectra of weakly bound van der Waals clusters have not yet been experimentally measured. Only an indirect determination[25,26] has resulted from the analysis of enhanced production of clusters of ^{4}He in terms of the successive stabilization of excited levels at growing values of the number of constituents of the clusters. The analysis of the partition function of parahydrogen clusters has revealed the existence of production enhancements at $N=13$, 31, and 36, in nice agreement with the experiment.[1] The effect is similar to the case of helium clusters, but the nature is very different. Instead of the stability threshold reason of helium clusters, here, the enhanced production is basically related to the existence of energy gaps in the excitations at the mentioned values of the number of constituents. There may be some corrections due to not including the $(n=1,L\neq 0)$ levels in the partition function. We expect, however, these effects to be small, as presumably such vibrational excitations would be some 20 K above the nonvibrational $(n=0,L)$ corresponding level.

ACKNOWLEDGMENTS

Stimulating conversations with S. Montero, M. Sevryuk, and J. P. Toennies are gratefully acknowledged. This work has been supported by MCyT (Spain) under Grant No. FIS2007-60138.

[1] G. Tejeda, J. M. Fernández, S. Montero, D. Blume, and J. P. Toennies, Phys. Rev. Lett. **92**, 223401 (2004).
[2] M. R. Hoare and P. Pal, Adv. Phys. **20**, 161 (1971).
[3] M. R. Hoare, Adv. Chem. Phys. **40**, 49 (1979).
[4] J. D. Honeycutt and H. C. Andersen, J. Phys. Chem. **91**, 4950 (1987).
[5] J. Jellinek, T. L. Beck, and R. S. Berry, J. Chem. Phys. **84**, 2783 (1986).
[6] A. L. Mackay, Acta Crystallogr. **15**, 916 (1962).
[7] F. Baletto and R. Ferrando, Rev. Mod. Phys. **77**, 317 (2005).
[8] Ph. Sindzingre, D. M. Ceperley, and M. L. Klein, Phys. Rev. Lett. **67**, 1871 (1991).
[9] S. Grebenev, B. Sartakov, J. P. Toennies, and A. F. Vilesov, Science **289**, 1532 (2000).
[10] Y. Kwon and K. B. Whaley, Phys. Rev. Lett. **89**, 273401 (2002).
[11] F. Paesani, R. E. Zillich, and K. B. Whaley, J. Chem. Phys. **119**, 11682 (2003).
[12] J. Tang and A. R. W. McKellar, J. Chem. Phys. **121**, 3087 (2004).
[13] F. Paesani, R. E. Zillich, Y. Kown, and K. B. Whaley, J. Chem. Phys. **122**, 181106 (2005).
[14] M. V. Rama Krishna and K. B. Whaley, Z. Phys. D: At., Mol. Clusters **20**, 223 (1991).
[15] M. A. McMahon, R. N. Barnett, and K. B. Whaley, J. Chem. Phys. **99**, 8818 (1993).
[16] M. A. McMahon and K. B. Whaley, Chem. Phys. **182**, 119 (1994).
[17] R. Guardiola and J. Navarro, Phys. Rev. A **74**, 025201 (2006).
[18] R. Guardiola and J. Navarro, Cent. Eur. J. Phys. **6**, 33 (2008).
[19] D. Scharf, M. L. Klein, and G. J. Martyna, J. Chem. Phys. **97**, 3590 (1992).
[20] F. Mezzacapo and M. Boninsegni, Phys. Rev. Lett. **97**, 045301 (2006).
[21] F. Mezzacapo and M. Boninsegni, Phys. Rev. A **75**, 033201 (2007).
[22] S. A. Khairallah, M. B. Sevryuk, D. M. Ceperley, and J. P. Toennies, Phys. Rev. Lett. **98**, 183401 (2007).
[23] S. Baroni and S. Moroni, ChemPhysChem **6**, 1884 (2005).
[24] J. E. Cuervo and P. N. Roy, J. Chem. Phys. **125**, 124314 (2006).
[25] R. Brühl, R. Guardiola, A. Kalinin, O. Kornilov, J. Navarro, T. Savas, and J. P. Toennies, Phys. Rev. Lett. **92**, 185301 (2004).
[26] R. Guardiola, O. Kornilov, J. Navarro, and J. P. Toennies, J. Chem. Phys. **124**, 084307 (2006).
[27] M. A. McMahon, R. N. Barnett, and K. B. Whaley, J. Chem. Phys. **99**, 8816 (1993).
[28] U. Buck, F. Huisken, A. Kohlhase, D. Otten, and J. Schaeffer, J. Chem. Phys. **78**, 4439 (1983).
[29] I. F. Silvera and V. V. Goldman, J. Chem. Phys. **69**, 4209 (1978).
[30] J. Boronat, in *Microscopic Approaches to Quantum Liquids in Confined Geometries*, edited by E. Krotscheck and J. Navarro (World Scientific, Singapore, 2002), Chap. 2, pp. 21–90.
[31] P. J. Reynolds, D. M. Ceperley, B. J. Alder, and W. A. Lester, Jr., J. Chem. Phys. **77**, 5593 (1982).
[32] O. Bohigas, A. M. Lane, and J. Martorell, Phys. Rep. **51**, 267 (1979).
[33] E. Lipparini and S. Stringari, Phys. Rep. **175**, 103 (1989).
[34] D. D. Frantz, J. Chem. Phys. **115**, 6136 (2001).
[35] L. S. Costa and D. C. Clary, J. Chem. Phys. **117**, 7512 (2002).
[36] J. Schaeffer and W. Meyer, J. Chem. Phys. **70**, 344 (1979).
[37] A. Watanabe and H. L. Welsh, Phys. Rev. Lett. **13**, 810 (1964).
[38] A. R. W. McKellar, J. Chem. Phys. **92**, 3261 (1990).
[39] A. R. W. McKellar, J. Chem. Phys. **95**, 3081 (1991).
[40] L. Rayleigh, Proc. R. Soc. London **29**, 71 (1879).
[41] A. Bohr and B. R. Mottelson, *Nuclear Structure, Nuclear Deformations, II* (World Scientific, Singapore, 1998), pp. 654–676.
[42] S. Stringari, in *The Chemical Physics of Atomic and Molecular Clusters*, edited by G. Scoles (North-Holland, Amsterdam, 1990), pp. 223–228.
[43] A. Tamura, Z. Phys. D: At., Mol. Clusters **40**, 225 (1997).
[44] D. J. Wales and J. P. K. Doye, J. Phys. Chem. A **101**, 5111 (1997) (coordinates of the clusters may be found in http://www-wales.ch.cam.ac.uk/CCD.html).